BASIC SCIENCE

Nanomedicine: Nanotechnology, Biology, and Medicine
29 (2020) 102245

Original Article

nanomedjournal.com

Deep convolutional neural networks combine Raman spectral signature of serum for prostate cancer bone metastases screening

Xiaoguang Shao, MD[a,1], Heng Zhang, PhD[b,1], Yanqing Wang, MD[a,1], Hongyang Qian, MD[a,1], Yinjie Zhu, MD[a], Baijun Dong, MD, PhD[a], Fan Xu, MD[a], Na Chen, PhD[b], Shupeng Liu, PhD[b,*], Jiahua Pan, MD, PhD[a,**], Wei Xue, MD, PhD[a,**]

[a]*Department of Urology, RenJi hospital, school of Medicine, Shanghai Jiao Tong University, Shanghai, People's Republic of China*
[b]*Shanghai Institute for Advanced Communication and Data science, Key laboratory of specialty Fiber Optics and Optical Access Networks, School of Communication and Information Engineering, Shanghai University, Shanghai, People's Republic of China*

Revised 27 May 2020

Abstract

Prostate cancer most frequently metastasizes to bone, resulting in abnormal bone metabolism and the release of components into the blood stream. Here, we evaluated the capacity of convolutional neural networks (CNNs) to use Raman data for screening of prostate cancer bone metastases. We used label-free surface-enhanced Raman spectroscopy (SERS) to collect 1281 serum Raman spectra from 427 patients with prostate cancer, and then we constructed a CNN based on LetNet-5 to recognize prostate cancer patients with bone metastases. We then used 5-fold cross-validation method to train and test the CNN model and evaluated its actual performance. Our CNN model for bone metastases detection revealed a mean training accuracy of 99.51% ± 0.23%, mean testing accuracy of 81.70% ± 2.83%, mean testing sensitivity of 80.63% ± 5.07%, and mean testing specificity of 82.82% ± 2.94%.

Key words: Raman spectroscopy; Prostatic neoplasms; Bone metastasis; Convolutional neural networks

The incidence of prostate cancer (PCA) in China has increased with an annual rate of 12.1% in recent years.[1] Bone metastases (BMs) are common during the course of PCA and occur in 8%-35% of newly diagnosed cancers. BMs reduce the quality of life and overall survival and are correlated with the following treatment strategies.[2] Radionuclide bone scan (BS) is commonly used to detect BMs. However, its disadvantages, including low specificity, high cost, and radioactive injury, cannot be ignored.[3] To reduce unnecessary examinations, guidelines based on baseline clinical parameters have been created to identify patients who need BS.[4,5] Therefore, rapid, inexpensive, and noninvasive laboratory tests to supplement BS would be useful.

During the BM process, metastases destroy bone structure and balance osteoblastic and osteolytic processes, resulting in abnormal bone metabolism. Components from bone metabolism are released into the bloodstream and can be serum markers for BM screening.[6] For example, bone formation markers are products of the osteoblastic process, including procollagen N-terminal propeptides (PIPNs), osteocalcin, and bone-specific-alkaline phosphatase (BAP). Bone resorption markers are the

This study was supported by National Natural Science Foundation of China (81572536, 81672850, 81772742, 81702840, 81702542, 81972578, 81902863), Science and Technology Commission of Shanghai Municipality (16411969800, 19411967400, 19ZR1431000, 19XD1402300, 19YF1428400), the Joint Research Foundation for Innovative Medical Technology of Shanghai Shenkang Hospital Development Center (16CR3049A), Shanghai Municipal Health Commission (201640247, 2019LJ11), Shanghai Municipal Education Commission-Gaofeng Clinical Medicine Grant Support (20152215 20191906).

Declaration of competing interest

*Correspondence to: S. Liu, Shanghai Institute for Advanced Communication and Data Science, Key Laboratory of Specialty Fiber Optics and Optical Access Networks, School of Communication and Information Engineering, Shanghai University, Shanghai, People's Republic of China.

**Corresponding authors at: Department of Urology, Ren Ji Hospital, School of Medicine, Shanghai Jiao Tong University, Shanghai, 200127, People's Republic of China.

E-mail addresses: liusp@shu.edu.cn (S. Liu), jiahua.pan@outlook.com (J. Pan), uroxuewei@163.com (W. Xue).

[1] These authors contributed equally to this work.

https://doi.org/10.1016/j.nano.2020.102245
1549-9634/

product of skeletal collagen degradation, such as pyridinoline, deoxypyridinoline, and bone sialoprotein. Numerous studies have assessed the diagnostic efficacy of these markers for BM in PCA.[7–9] However, these markers are still not recommended for routine clinical use because the results are often contradictory perhaps because of poor analytical tools. Therefore, it might be useful to develop a method to extract holistic information from blood components for BM detection.

Surface-enhanced Raman spectroscopy (SERS) has emerged as a powerful technique for blood analysis. It offers a quick response, high sensitivity/specificity, and data fingerprint unique to the molecules' structure.[10] Our group also reported that SERS could detect PCA and predict disease recurrence by analyzing blood and expressed prostatic secretion.[11–13] However, Raman spectra contain complex peaks that reveal the molecular information of biological samples. It is still challenging to identify the underlying explanatory factors in complex spectra and develop a practical classification model based on Raman spectra. Recently, convolutional neural networks (CNNs) have led to breakthrough results in many tasks, such as image classification and cancer diagnosis.[14,15] CNN is an artificial neural network that can mimic the pattern of human brain in message processing. It can extract features from input data through several channels of convolutions and form filtered output features for classification. CNNs have also been used for Raman spectrum recognition with high accuracy.[16,17]

Here, we studied the capacity of CNN to use Raman spectra from human serum to screen for prostate cancer BM. We collected serum Raman spectra from patients with PCA with or without BM as training and testing datasets. We then used a 5-fold cross-validation method to train and test the CNN model and evaluated the system's actual performance.

Methods

Study population and sample collection

We enrolled patients with PCA from July 2014 to April 2019 in our medical center. Patients were included according to criteria below: 1) diagnosed with PCA by prostate biopsy, 2) underwent a Tc 99m MDP bone scan, and suspicious lesions were confirmed with magnetic resonance imaging (MRI), and 3) no drug treatment before blood collection. This study was approved by the Institutional Ethics Committee of the Ren Ji Hospital affiliated to the Shanghai Jiao Tong University, School of Medicine (approval no. Renji/ 2013126). After 12 h of overnight fasting, 5 ml of blood was collected from the patients. The blood was centrifuged at 3000 ×*g* for 5 min, and serum was collected and frozen at −80 °C until SERS analysis.

Silver nanoparticles (Ag NPs) synthesis

Ag NPs were prepared via the sodium citrate reduction method as previously reported.[12] Briefly, 1 ml of a 0.1 M $AgNO_3$ solution was added to 99 ml of deionized water. After the solution was boiled, 1.8 ml of 1% sodium citrate tribasic solution was added. The solution was boiled until its color became blue/green. The Ag NPs solution was concentrated at 6000 rpm for 10 min, and the final 1 ml of concentrate was used for SERS measurements. The Ag NPs were characterized by transmission electron microscopy (TEM) (JEOL, JEM-100CX, Tokyo, Japan).

SERS measurement and data processing

First, 10 μL of serum was mixed with 10 μL of Ag NPs solution, and the mixture was incubated at room temperature for 5 min and then transferred onto a silicon plate for Raman data collection. A confocal Raman microscope (LabRAM HR Evolution, Horiba, France) was used to analyze the serum samples. An yttrium aluminum-garnet (Nd: YAG) laser (λ = 532 nm) was focused onto the sample with a micro-objective (50×, NA = 0.75) to excite Raman spectra. The measurement parameters were as follows: 600 g mm^{-1} grating, 100-μm confocal hole, 1 s of acquisition time, and 400-1800 cm^{-1} spectral interval. Three spots were analyzed of each sample to get representative Raman spectra of the serum.

The Raman spectra were acquired using LabSpec 6 software (Horiba). The fluorescence background in the raw data was removed using a Vancouver Raman algorithm based on the fifth-order polynomial fitting method.[18] The spectra were then normalized by the max–min approach.

CNN model construction

We designed a CNN model based on LetNet-5, which is a classical CNN architecture for handwriting recognition. The CNN model included two alternate convolution layers and two pooling layers for features extraction. Those extracted features were operated by fully connected layers and Softmax output layer, which could be viewed as a classifier. To make the CNN model suitable for Raman spectral data, the input layer, convolution layers, and pooling layers were designed as a one-dimensional linear structure. The model was optimized with Adam optimizer while the loss function was set as cross-entropy. The learning rate was 0.005. The proposed CNN was implemented using Keras and Tensorflow.

CNN model evaluation

The CNN model was trained and validated using Raman spectra from patients with PCA in our study. A 5-fold cross-validation was performed for the CNN model at each epoch (Figure 3, *B*). Briefly, the entire Raman spectra data were randomly divided into training and test datasets for CNN training and validation. The ratio of training and test datasets was set to be 4:1. The CNN training and validation procedure was conducted repeatedly until all of the data were trained and tested.

The sensitivity, specificity, and accuracy were calculated to evaluate the performance of the CNN models. Continuous variables were compared with Student's *t* test or Mann-Whitney *U* test and expressed as the mean (SD). Categorical variables were compared with Fisher's exact test. A two-sided *P* value of < 0.05 was considered to be statistically significant. Principal component analysis and linear discriminate analysis (PCA-LDA), principal component analysis and logistic regression (PCA-LR) and support vector machine (SVM) were performed using MATLAB R2017a (MathWorks, Natick, USA) and SPSS version 25.0 (IBM Corp, New York, USA).

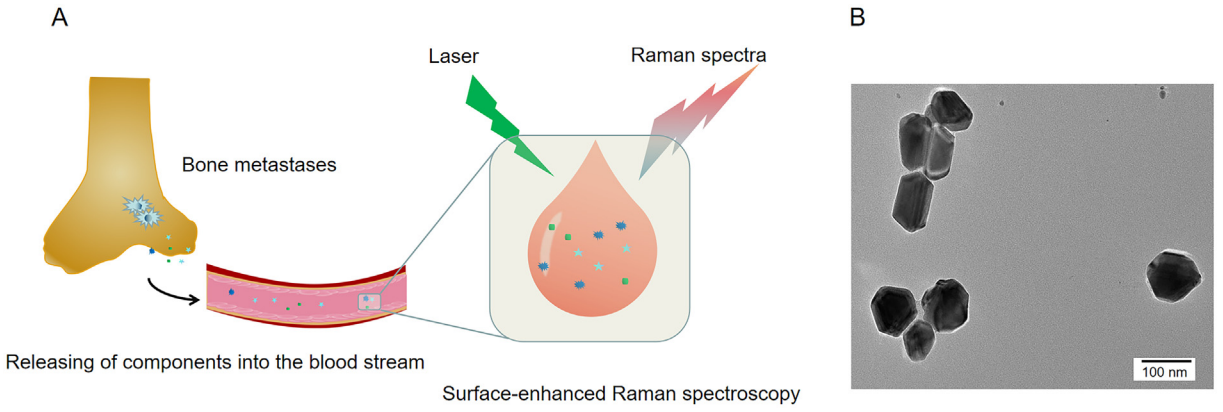

Figure 1. **(A)** Schematic diagram of SERS detection of abnormal metabolism during bone metastases. **(B)** TEM image of Ag nanoparticles.

Results

A total of 427 patients with PCA were included in this study, including 204 patients diagnosed with BM; 223 did not have BM. Table S1 shows that the clinical features of the two groups of patients were significantly different. Compared to patients without BM, the patients with BM had higher serum PSA levels (P<0.01), higher pathologic Gleason scores (P<0.01), a higher proportion of positive biopsies (P<0.01), and advanced clinical stage (P<0.01). However, the age between the two patient groups had no significant difference (P=0.38).

Figure 1, *A* demonstrates the schematic of SERS detection of abnormal metabolism during bone metastases, while Figure 1, *B* shows TEM data for the Ag nanoparticles with a diameter of 100 nm.

SERS spectral signature of serum

A total of 1281 SERS spectra were obtained from patients with PCA. The mean serum Raman spectra with their standard deviation are shown in Figure 2. The PCA patients with and without BM showed similar Raman spectral signature of serum: Both contained the following Raman peaks with tentative biochemical assignments[19,20]: 635 cm^{-1} (C-S twist/l-tyrosine); 724 cm^{-1} (CH bending vibration/adenine, hypoxanthine); 811 cm^{-1} (C-C-O stretching vibration/L-serine); 1009 cm^{-1} (C-H

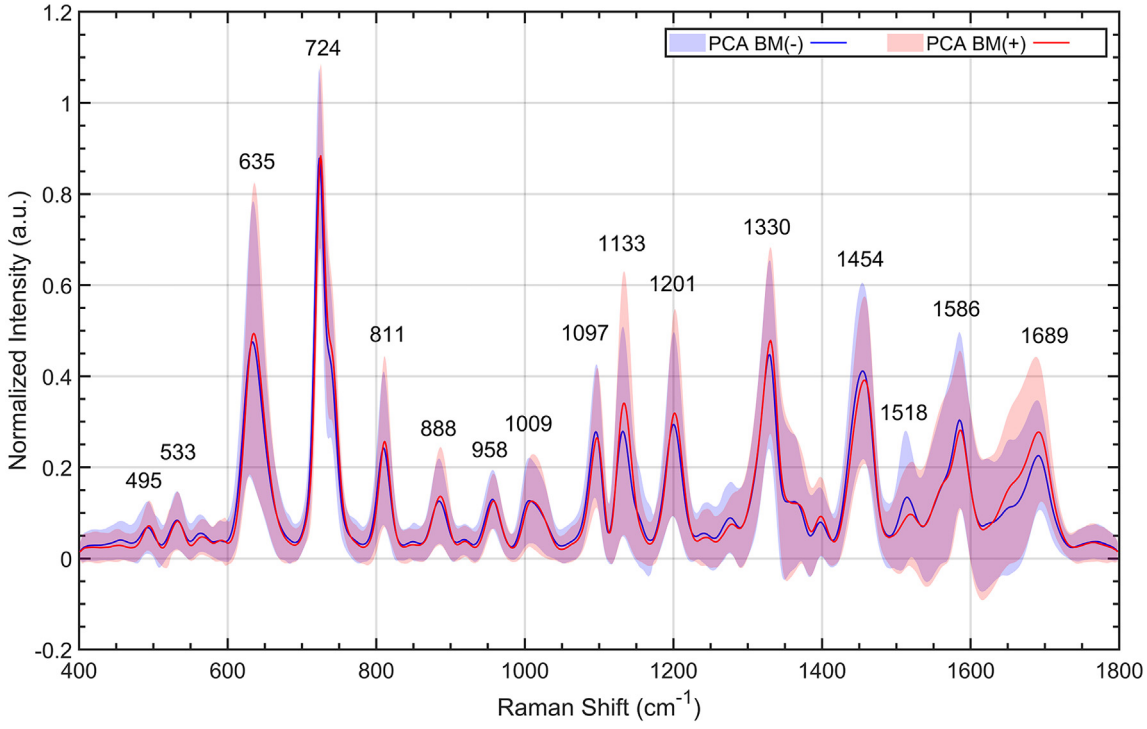

Figure 2. Normalized mean SERS spectra of serum from 204 PCA patients with BM and 223 patients without BM. The solid lines represent the mean spectra, while the gray zones represent the standard deviation.

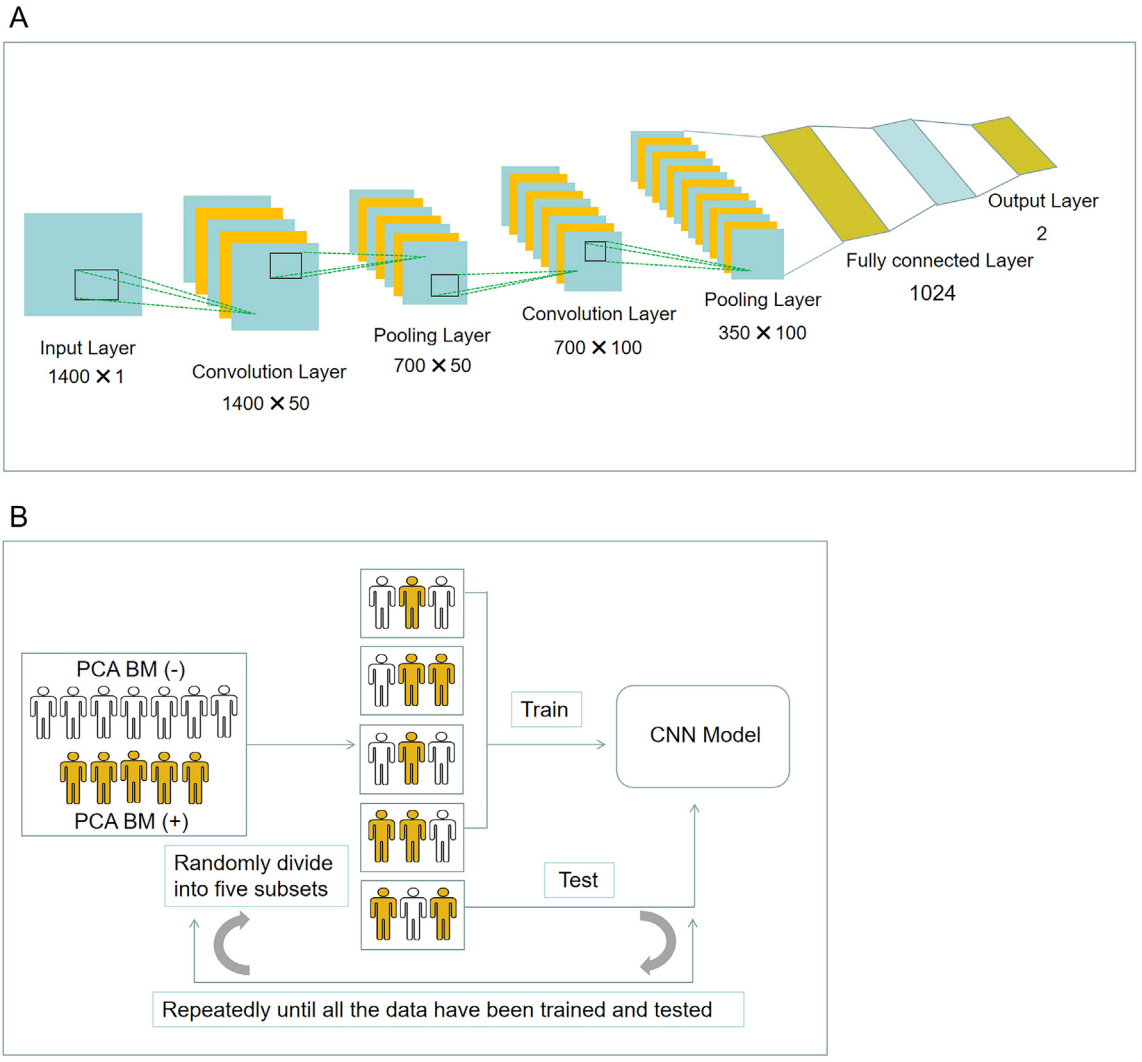

Figure 3. **(A)** Structure of CNN model constructed in this study. The numbers represent the node numbers of each layer. **(B)** Procedure of 5-fold cross-validation in CNN model training and testing.

stretching vibration/phenylalanine); 1330 cm^{-1} (CH_2 twist vibration/lipids and C–H vibration in DNA/RNA); 1586 cm^{-1} (C=C bending/acetoacetate); and 1689 cm^{-1} (C=C stretching vibration/amide I). However, The PCA patients with BM only showed stronger Raman intensity in peak 1133 cm^{-1} (C-N stretching vibration/d-mannose) and peak 1689 cm^{-1} (C=C stretching vibration/amide I) than patients without BM. Those Raman peaks were mostly identified as the amide I band in collagen.[19]

CNN model construction and evaluation

We constructed a CNN model based on LetNet-5. Figure 3, *A* shows a schematic structure of our CNN model, including seven layers. The input layer was used for data input with 1400 nodes. The first convolution layer was used to extract 50 characters from the Raman spectra with a node number of 1400*50 and kernel size of 1*12. The pooling layer was used to compress previous layer data to 700*50 with pool size of 1*2 and stride of [0,2]. The next convolutional layer contained a node number of 1400*50 and a kernel size of 1*12, which extracted 100 characters from the previous layer. The next pooling layer was used to compress the previous layer data to 350*100 with a pool size of 1*2 and stride of [0,2]. The fully connected layer and output layer were used for classification.

In each epoch, we used preprocessed Raman data and a 5-fold cross-validation method to train and test CNN model for BM recognition. The training and testing accuracies in each epoch were calculated, and the results are shown in Figure 4, *A*. As the epoch grew, the training accuracy increased to almost 100%. However, the mean testing accuracy varied across different epochs. The testing results indicated that the CNN model showed the best performance when the epoch reached 57. The results are shown in Figure 4, *B*, and the CNN model had a mean training accuracy of 99.51% ± 0.23%, mean testing accuracy of 81.7% ± 2.83%, mean testing sensitivity of 80.63% ± 5.07%, and mean testing specificity of 82.82% ± 2.94%.

To further evaluate the performance of our model, we compared it with several typical traditional algorithms including

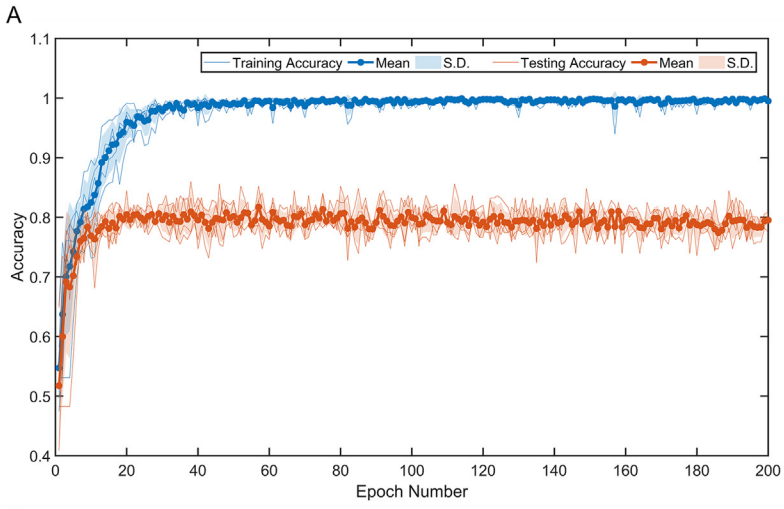

Performance at 57 epoch of CNN model	
Mean Training Accuracy	99.51% ± 0.23%
Mean Testing Accuracy	81.70% ± 2.83%
Mean Testing Sensitivity	80.63% ± 5.07%
Mean Testing Specificity	82.82% ± 2.94%

Figure 4. **(A)** The training and testing accuracy in each epoch of CNN. The line with dots represents the mean accuracy, while the gray zones represent the standard deviation in every testing–training course of 5-fold cross-validation. **(B)** The best performance of CNN model for BM recognition at 57 epochs. Graphs and table show the mean training accuracy, mean testing accuracy, mean testing sensitivity and mean testing specificity.

principal component analysis and linear discriminate analysis (PCA-LDA) and principal component analysis and logistic regression (PCA-LR). As shown in Figures S1 and S2, these methods revealed testing accuracy of 76.17% ± 3.28% and 77.03% ± 2.84%, respectively. We also compared our model to support vector machine (SVM), a typical traditional machine learning algorithm. As shown in Figure S3, the SVM exhibited testing accuracy of 56.77% ± 2.21%

Discussion

Prostate cancer frequently metastasizes to bone.[21] Although the underlying mechanisms are still unclear, it is important to identify those patients suffering from BM. Bone scanning is widely used to detect BM despite its low specificity and high cost.[3] MRI has higher efficacy in BM detection; however, it is time-consuming and expensive.[22] Therefore, a rapid, inexpensive, and noninvasive method to supplement BS is needed. Here, we used SERS to collect a Raman spectral signature of serum and then developed a CNN model to extract features of the Raman spectra and recognize PCA patients with BM. We then used a 5-fold cross-validation method to train and test the CNN model. The results showed that the CNN model could identify PCA patients with BM with sensitivity of 80.63% ± 5.07%, specificity of 82.82% ± 2.94% and accuracy of 81.70% ± 2.83%.

Many studies have reported that SERS is a promising technique for biofluid analysis, including blood,[20] urine,[23] saliva,[24] and cerebrospinal fluid.[25] SERS provides the intrinsic spectra of biofluids and classifies various diseases. In prostate cancer, label-free SERS has been reported to detect and monitor disease via analysis of serum,[13,26] urine,[23] and prostatic secretions.[12] Although these studies have demonstrated encouraging preliminary results in terms of accuracy, several aspects require improvements before SERS can be considered in mainstream medicine. First, the SERS signal is often complex and variable due to the complex composition of the biofluid;

thus, reliable quantitative results are often lacking. Moreover, given the inter- and intra-individual variability, more subjects are often needed to achieve reasonable results. In addition, it is necessary to develop a practical classification model that can be used to classify new spectral data.

Here, we enrolled 427 patients with PCA and collected 1281 Raman spectra. We presented these data as mean and standard deviation to show the spectral signature of patients with PCA. These Raman spectra had similar Raman peaks with variable intensities in different subjects. This indicates that we collected reliable spectra in our study with the same experimental settings. Although previous studies reported that BM metastases could change the components in the blood,[6] we found that the variation in the Raman spectra of serum between PCA patients with and without BM was minimal. The PCA patients with BM only showed stronger Raman intensity than patients without BM in peak 1133 cm^{-1} (C-N stretching vibration/d-mannose) and peak 1689 cm^{-1} (C=C stretching vibration/amide I).[27] The Raman peak 1689 cm^{-1} was mostly attributed to the collagen, which could originate from bone matrix destruction and skeletal collagen degradation during BM process.[6]

We next explored a method to extract features from the Raman spectra and developed a practical classification model. CNN is an advanced deep learning method with good performance at recognizing two-dimensional data. CNN has been used in lesion detection,[28] classification,[29] and stimulated Raman scattering image recognition.[30] CNN has also been used to evaluate Raman spectra with higher accuracy than previous statistical methods.[16,17]

Here, we designed a CNN model to recognize serum Raman spectra from patients with PCA and classified those patients with BM. We constructed a CNN model via LetNet-5, which is a classical CNN architecture for handwriting recognition. We also combined convolution layers and pooling layers into a one-dimensional linear structure to make them suitable for Raman spectral data.

CNN works best with large amounts of data. We used 1281 datasets with 5-fold cross validation to train and test the CNN model in each epoch. We then evaluated its diagnostic performance in every training–testing course. Figure 3, *B* shows that the training accuracy increased to almost 100% with growing epoch procedures. This indicated the over-fitting problem during the algorithm training. However, the testing procedure modified this problem and demonstrated the actual accuracy of the CNN model. The mean testing accuracy varied at different epochs. The CNN model had the best performance when the epoch arrived at 57. These conditions led to a mean training accuracy of 99.51% ± 0.23%, mean testing accuracy of 81.7% ± 2.83%, mean testing sensitivity of 80.63% ± 5.07%, and mean testing specificity of 82.82% ± 2.94%. When we compared our model with several typical traditional machine learning algorithms, including PCA-LDA, PCA-LR and SVM, we found that our model more accurately detected BM through investigating Raman spectra. Consequently, our model showed better performance of BM detection than other traditional algorithms.

Although these results indicated the potential value of our model in BM screening, the accuracy of this model is a little lower than previously reported CNN studies.[14] This might be due to the relatively small number of spectral data used here for training. In principle, a larger database leads to a deeper neural network.[30] Our CNN model can be improved with larger datasets in the future. This study was also done in a single center and can be improved when data are obtained from other medical centers.

In conclusion, we showed SERS analysis of serum integrated with a CNN model to help identify PCA patients with BM. Larger datasets will improve the model for rapid and automated BM screening to supplement PCA bone scans.

Appendix A. Supplementary data

Supplementary data to this article can be found online at https://doi.org/10.1016/j.nano.2020.102245.

References

1. Chen W, Zheng R, Baade PD, Zhang S, Zeng H, Bray F, et al. Cancer statistics in China, 2015. *CA Cancer J Clin* 2016;**66**:115.
2. Norgaard M, Jensen AO, Jacobsen JB, Cetin K, Fryzek JP, Sørensen HT. Skeletal related events, bone metastasis and survival of prostate cancer: a population based cohort study in Denmark (1999 to 2007).J Urol 2010;**184:** 162.
3. Merdan S, Womble PR, Miller DC, Barnett C, Ye ZJ, Linsell SM, et al. Toward better use of bone scans among men with early-stage prostate cancer. *Urology* 2014;**84**:793.
4. Briganti A, Passoni N, Ferrari M, Capitanio U, Suardi N, Gallina A. et al. When to perform bone scan in patients with newly diagnosed prostate cancer: external validation of the currently available guidelines and proposal of a novel risk stratification tool.Eur Urol 2010;**57:** 551.
5. Cornford P, Bellmunt J, Bolla M, Briers E, De Santis M, Gross T, et al. EAU-ESTRO-SIOG guidelines on prostate cancer. Part II: treatment of relapsing, metastatic, and castration-resistant prostate cancer. *Eur Urol* 2017;**71**:630.
6. Jung K, Lein M. Bone turnover markers in serum and urine as diagnostic, prognostic and monitoring biomarkers of bone metastasis. *Biochim Biophys Acta* 2014;**1846**:425.
7. Kamiya N, Suzuki H, Yano M, Endo T, Takano M, Komaru A, et al. Implications of serum bone turnover markers in prostate cancer patients with bone metastasis. *Urology* 2010;**75**:1446.
8. Wei RJ, Li TY, Yang XC, Jia N, Yang XL, Song HB, et al. Serum levels of PSA, ALP, ICTP, and BSP in prostate cancer patients and the significance of ROC curve in the diagnosis of prostate cancer bone metastases. *Genet Mol Res* 2016;**15**.
9. Lara PN, Jr., Ely B, Quinn DI, Mack PC, Tangen C, Gertz E. et al. Serum biomarkers of bone metabolism in castration-resistant prostate cancer patients with skeletal metastases: results from SWOG 0421.J Natl Cancer Inst 2014;**106:** dju013.
10. Zhang Y, Mi X, Tan X, Xiang R. Recent progress on liquid biopsy analysis using surface-enhanced Raman spectroscopy. *Theranostics* 2019;**9**:491.
11. Chen N, Rong M, Shao X, Zhang H, Liu S, Dong B. et al. Surface-enhanced Raman spectroscopy of serum accurately detects prostate cancer in patients with prostate-specific antigen levels of 4-10 ng/mL. Int J Nanomedicine 2017;**12:** 5399.
12. Shao X, Pan J, Wang Y, Zhu Y, Xu F, Shangguan X, et al. Evaluation of expressed prostatic secretion and serum using surface-enhanced Raman spectroscopy for the noninvasive detection of prostate cancer, a preliminary study. *Nanomedicine* 2017;**13**:1051.

13. Pan J, Shao X, Zhu Y, Dong B, Wang Y, Kang X, et al. Surface-enhanced Raman spectroscopy before radical prostatectomy predicts biochemical recurrence better than CAPRA-S. *Int J Nanomedicine* 2019;**14**:431.
14. Yamashita R, Nishio M, Do RKG, Togashi K, et al. Convolutional neural networks: an overview and application in radiology. *Insights Imaging* 2018;**9**:611.
15. Coudray N, Ocampo PS, Sakellaropoulos T, Narula N, Snuderl M, Fenyö D, et al. Classification and mutation prediction from non-small cell lung cancer histopathology images using deep learning. *Nat Med* 2018;**24**:1559.
16. Acquarelli J, van Laarhoven T, Gerretzen J, Tran TN, Buydens LMC, Marchiori E. Convolutional neural networks for vibrational spectroscopic data analysis. *Anal Chim Acta* 2017;**954**:22.
17. Liu J, Osadchy M, Ashton L, Foster M, Solomon CJ, Gibson SJ. Deep convolutional neural networks for Raman spectrum recognition: a unified solution. *Analyst* 2017;**142**:4067.
18. Huang Z, McWilliams A, Lui H, McLean DI, Lam S, Zeng H. Near-infrared Raman spectroscopy for optical diagnosis of lung cancer. *Int J Cancer* 2003;**107**:1047.
19. Shao L, Zhang A, Rong Z, Wang C, Jia X, Zhang K. Fast and non-invasive serum detection technology based on surface-enhanced Raman spectroscopy and multivariate statistical analysis for liver disease. *Nanomedicine* 2018;**14**:451.
20. Vargas-Obieta E, Martinez-Espinosa JC, Martinez-Zerega BE, Jave-Suárez LF, Aguilar-Lemarroy A, González-Solís JL. Breast cancer detection based on serum sample surface enhanced Raman spectroscopy. *Lasers Med Sci* 2016;**31**:1317.
21. Coleman RE: Clinical features of metastatic bone disease and risk of skeletal morbidity. Clin Cancer Res 2006;**12:** 6243s.
22. Lecouvet FE, El Mouedden J, Collette L, Coche E, Danse E, Jamar F, et al. Can whole-body magnetic resonance imaging with diffusion-weighted imaging replace Tc 99m bone scanning and computed tomography for single-step detection of metastases in patients with high-risk prostate cancer? *Eur Urol* 2012;**62**:68.
23. Del Mistro G, Cervo S, Mansutti E, Spizzo R, Colombatti A, Belmonte P, et al. Surface-enhanced Raman spectroscopy of urine for prostate cancer detection: a preliminary study. *Anal Bioanal Chem* 2015;**407**:3271.
24. Feng S, Huang S, Lin D, Chen G, Xu Y, Li Y, et al. Surface-enhanced Raman spectroscopy of saliva proteins for the noninvasive differentiation of benign and malignant breast tumors. *Int J Nanomedicine* 2015;**10**:537.
25. Sathyavathi R, Dingari NC, Barman I, Prasad PS, Prabhakar S, Narayana Rao D, et al. Raman spectroscopy provides a powerful, rapid diagnostic tool for the detection of tuberculous meningitis in ex vivo cerebrospinal fluid samples. *J Biophotonics* 2013;**6**:567.
26. Zhou L, Liu Y, Wang F, Jia Z, Zhou J, Jiang T, et al. Classification analyses for prostate cancer, benign prostate hyperplasia and healthy subjects by SERS-based immunoassay of multiple tumour markers. *Talanta* 2018;**188**:238.
27. Westley C, Xu Y, Thilaganathan B, Carnell AJ, Turner NJ, Goodacre R. Absolute quantification of uric acid in human urine using surface enhanced Raman scattering with the standard addition method. *Anal Chem* 2017;**89**:2472.
28. Lakhani P. Sundaram B: Deep learning at chest radiography: automated classification of pulmonary tuberculosis by using convolutional neural networks. *Radiology* 2017;**284**:574.
29. Yasaka K, Akai H, Abe O, Kiryu S. Deep learning with convolutional neural network for differentiation of liver masses at dynamic contrast-enhanced CT: a preliminary study. *Radiology* 2018;**286**:887.
30. Zhang L, Wu Y, Zheng B, Su L, Chen Y, Ma S, et al. Rapid histology of laryngeal squamous cell carcinoma with deep-learning based stimulated Raman scattering microscopy. *Theranostics* 2019;**9**:2541.